Proceedings World Geothermal Congress 2026
Calgary, Canada, June 8 – 11, 2026

Preliminary Structural Characterization of a Fractured Granite Targeted for Geothermal and Lithium Brine Extraction

Samuel Grainger[1*], David McNamara[1], Elisabetta Mariani[1], Robin Shail[2], Chris Yeomans[3], Will McKenzie[4]
University of Liverpool[1*], University of Exeter[2], Neo Geo Consulting Ltd[3], Cornish Lithium Plc[4]
Samuel.grainger@liverpool.ac.uk

Keywords: Structural geology, Geothermal exploration, Granite-hosted reservoir, Fault zone, Permeability anisotropy, Lithium, Fracture networks

ABSTRACT

The Porthgwarra-Land's End Fault Zone (PLFZ) in Southwest England provides a surface analogue for steeply dipping faults in the subsurface that host geothermal brines enriched in dissolved lithium. These structures host geothermal waters and are targeted at depths of 2–5 km for heat and/or power and lithium production due to their elevated permeability relative to the surrounding host rock. Using integrated field observations and systematic fracture data collection, this study addresses the structural architecture and inferred permeability of the PLFZ. In the study area, the PLFZ comprises four principal strands with fault cores composed of gouge, mechanical and hydrothermal breccias, and epithermal quartz–hematite veins. Kinematic indicators preserved on fault surfaces and in fault rocks suggest distinct episodes of oblique-slip and strike-slip displacement. Fracture data reveal a heterogeneous and anisotropic permeability structure. The fracture-dense damage zone promotes fault-parallel flow and sealed fault cores act as barriers to cross-fault fluid flow. These findings provide a preliminary understanding of the influence of fault architecture on permeability anisotropy in a granite-hosted geothermal reservoir. The results provide a field-scale analogue of a subsurface target for geothermal and critical-metal exploration in the Cornubian Batholith and may be applied to similar projects worldwide.

1 INTRODUCTION

Fault and fracture networks are crucial for fluid storage and fluid flow in geothermal reservoirs, particularly those hosted within rocks of low permeability (Bertrand et al., 2015, Evans et al., 2025). Accurately mapping faults and fracture networks is therefore essential for predicting permeability and fluid flow in the crust, and modelling geothermal systems (Caine et al., 1996, Sibson, 2000, Sibson, 2001, Mitchell and Faulkner, 2012, Liotta et al., 2021). The spatial and temporal evolution of fault zone permeability is highly variable dependent on rock type, fault architecture, deformation mechanisms and the earthquake cycle (Sibson, 1990, Caine et al., 1996, Mitchell and Faulkner, 2012). The damage zones of faults, particularly within the hanging wall, often have a high fracture intensity and therefore enhanced permeability (Kurz et al., 2008, Wibberley et al., 2008). Faults tend to act as fluid conduits parallel to the fault plane, developing channels particularly in the strike and dip directions. Conversely, they restrict flow perpendicular to the fault plane due to the occurrence of impermeable fault rocks within the fault core (Caine et al., 1996, Faulkner et al., 2010). Fracture orientation relative to the contemporary *in situ* stress field is a critical factor controlling fluid flow in a fault zone (Barton et al., 1995, Faulkner and Armitage, 2013, Ferrill et al., 2020). Fractures subject to lower normal stresses have a higher dilation tendency, and therefore greater aperture. Consequently, when fractures are present in this orientation, permeability on the σ_1–σ_2 plane (perpendicular to the σ_3 stress direction) is relatively enhanced (Ferrill et al., 2020). The aperture of a fracture is not only a function of dilation tendency and can be influenced by the mode and rate of opening, mineralization, gouge and clay fill and fracture roughness (Bense et al., 2013). The connectivity of permeable fractures is a critical control on fluid flow in the fracture network (Bense et al., 2013, Sanderson and Nixon, 2018). The connectivity of fractures is, in turn, controlled by the fracture intensity and fracture length, requiring systematic fracture data to constrain it.

The relationship between stress, fracture orientation, and permeability is of relevance to the Cornubian high heat-producing granite batholith in Southwest England, which is a significant geothermal resource (Beamish and Busby, 2016, Turan et al., 2024). Exploration and development activity is ongoing and the first power production occurred in February 2026 (Ledingham et al., 2019, Reinecker et al., 2021, Olver and Law, 2025), alongside efforts to extract lithium from the geothermal waters (Shaw, 2022). The principal exploration targets at depths of 2–5 km are NW–SE-striking faults known locally as 'crosscourses'. They are targeted due to their enhanced permeability (Reinecker et al., 2021). Historically, this regional mining term describes faults that intersect granite-related Sn-Cu mineral veins at a high angle, typically causing dextral separation. Crosscourse fracture systems often host epithermal mineralization, reflecting the Triassic migration of basinal brines through granites

and their host rocks (Dominy et al., 1994, Scrivener et al., 1994, Andersen et al., 2016), and are associated with host rock alteration (Inskip et al., 2023). No comprehensive structural analysis of crosscourse faults has been undertaken, and consequently crosscourse network permeability characteristics remain poorly constrained. The aim of this study is to develop an understanding of how structural architecture influences fluid flow in geothermal surface analogues, improving predictions of permeability in deeper, fault-controlled geothermal systems.

2 METHODS AND MATERIALS

This study carried out structural mapping of a key field area that contains the surface expression of the Porthgwarra-Land's End Fault Zone (PLFZ) hosted by the Land's End Granite, within the Early Permian Cornubian Batholith. The batholith was emplaced into Devonian and Carboniferous metasedimentary successions (Figure 1; Leveridge et al., 1990, Leveridge and Hartley, 2006, Shail and Leveridge, 2009). The PLFZ is an anastomosing structure with exposures at several coastal locations between Porthgwarra and Land's End. In this study it is used as an analogue for similar crosscourse fault zones at depth.

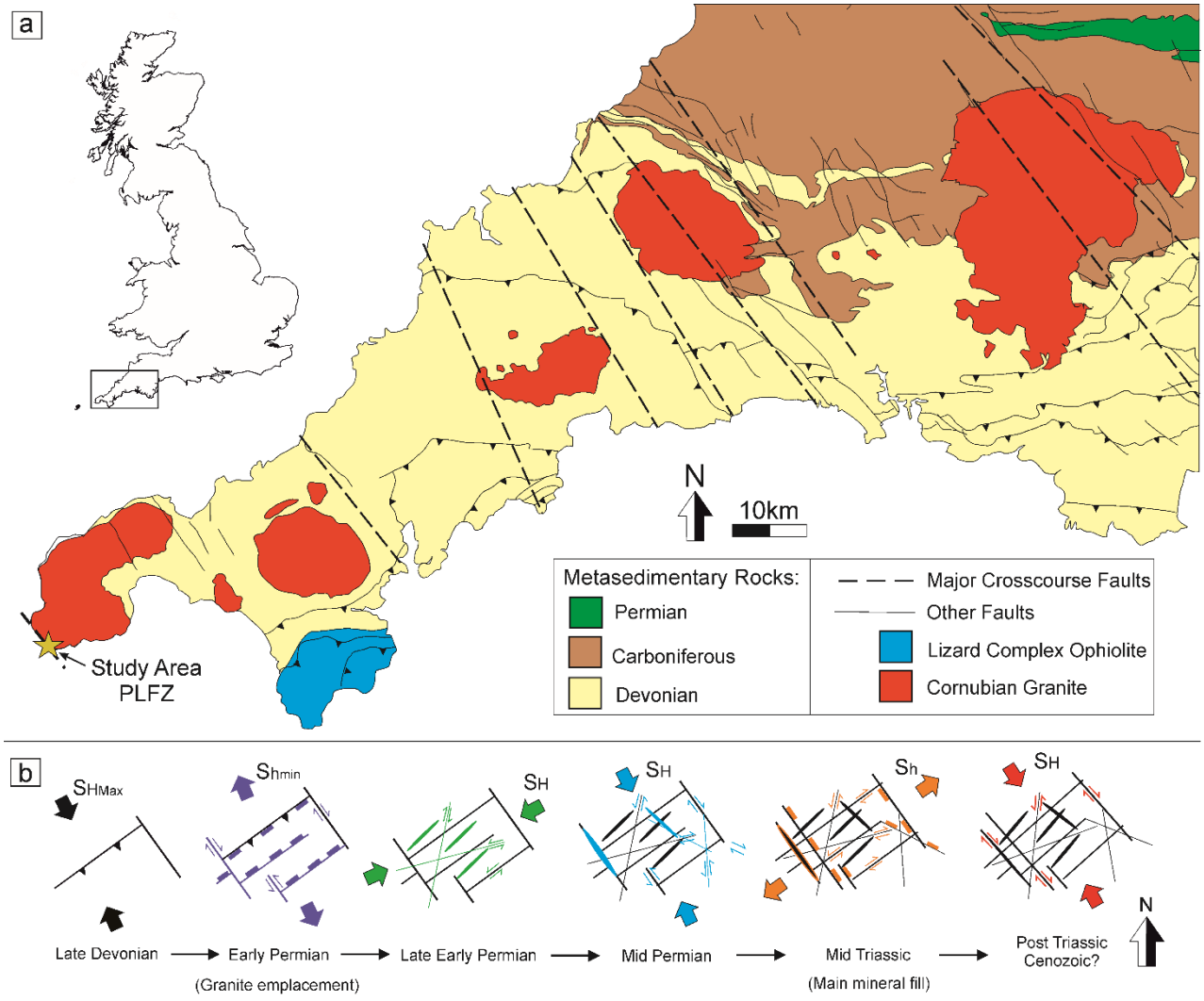


Figure 1. a: Geological map of Southwest England with the study area shown by a gold star. Modified after Shail and Leveridge (2009) with supplementary fault data from Dearman (1963) and British Geological Survey (BGS) maps. The inset map (top left) shows the location of the study area within Great Britain. b: Map-view schematic of the tectonic development of fracture systems in Southwest England; modified after Shail and Alexander (1997).

NW–SE transfer faults in metasedimentary successions, formed during Rhenohercynian rifting (Chapman, 1989, Shail and Alexander, 1997), represent the precursors of crosscourse fault zones. These faults were repeatedly reactivated during later tectonic events, including the Variscan orogeny, latest Carboniferous–Early Permian extension, and Triassic rifting (Figure 1; Shail and Alexander, 1997, Leveridge and Hartley, 2006).

Permian–Triassic tectonism played a key role in crosscourse fault development and was accompanied by magmatism and fluid circulation. The Cornubian Batholith was emplaced during the Early Permian under a NNW-SSE extensional regime. This event released magmatic-hydrothermal fluids that migrated through fault and fracture networks, including NNW-SSE transfer faults. Within these networks, magmatic-hydrothermal fluids mixed with meteoric (± basinal) fluids to generate diverse W-Sn-Cu-Zn-Pb mineralization (Chen et al., 1993, Dominy et al., 1994, Gleeson et al., 2000). Triassic ENE-WSW extension reactivated these transfer faults (Figure 1) and formed new NNW-SSE striking extensional faults that controlled the migration of highly saline basinal brines, precipitating quartz–hematite veins with minor accessory minerals (Dominy et al., 1994, Gleeson et al., 2001, Andersen et al., 2016). Triassic epithermal quartz-hematite precipitate is the most abundant crosscourse fault fill, with sulfide minerals, clays, fluorite veins and breccias also described in previous studies (Dominy et al., 1994, Scrivener et al., 1994, Andersen et al., 2016).

Cenozoic intraplate shortening, controlled by Mid-Atlantic Ridge and Alpine/Pyrenean plate boundary stresses, caused strike-slip reactivation of NW–SE (dextral) and NNE–SSW (sinistral) oriented faults (Figure 1; Holloway and Chadwick, 1986, Nixon et al., 2011, Connolly et al., 2024). The current tectonic regime in England is strike-slip with vertical σ_2, NW–SE σ_1, and NE–SW σ_3 (Baptie, 2010). The NE–SW orientation of the minimum horizontal stress (σ_h) favors fluid flow along faults perpendicular to this orientation, hence the targeting focus on NW–SE aligned crosscourse faults during geothermal exploration (Reinecker et al., 2021).

Fieldwork to collect structural data and characterize the PLFZ was carried out in June 2025 at Pol Ledan Cove, near Porthgwarra, Cornwall. This coastal exposure is a cliff section, with limited foreshore platform exposure (Figure 2).



Figure 2: A drone scan of Pol Ledan Cove with Porthgwarra-Land's End fault cores colored red, surface deposits in green and yellow, and scanline locations indicated. Direction of observation given in bottom left.

Fault cores were described and fault orientations measured; systematic fracture data were collected using one 52.2 m linear scanline (1D transect) and four 2 m diameter circular scanlines (2D area) on the cliff sections of the exposure (Figure 2), using the workflow detailed by Watkins et al. (2015). The height of the linear scanline was 1 m above the base of the exposure for accessibility and consistent data collection. One circular scanline was carried out near Lamorna, with no nearby exposed fault. This circular scanline therefore represents a 'background' measurement. The linear scanline trace location was chosen for its varying exposure orientations and inclusion of both hanging wall and footwall regions of a major fault core. Circular scanline locations were chosen in relatively flat regions of cliff exposure to sample a plane and all were limited to 2 m diameter because of access restrictions.

For fractures encountered on linear scanlines, distance from origin, orientation, spacing, thickness, aperture at scanline intercept, alteration, and fill were measured. For fractures intercepting circular scanlines, orientation, spacing, thickness and aperture at scanline intercept, alteration, and fill were measured (Figure 3).

The fracture data are subject to sampling bias, particularly for dip angles. Of the 156 fractures recorded, 115 were recorded on the horizontal linear scanline causing underrepresentation of gently-dipping fractures. Strike orientation bias from the linear scanline is present but reduced because of the variable orientations of measured sections and the application of Terzaghi (1965) corrections. Circular scanlines also have some sampling bias with fractures similarly oriented to the sampling plane underrepresented, i.e. steeply dipping fractures in this study. The two scanline techniques are complementary and together provide a reasonable estimation of fracture distribution in the study area.

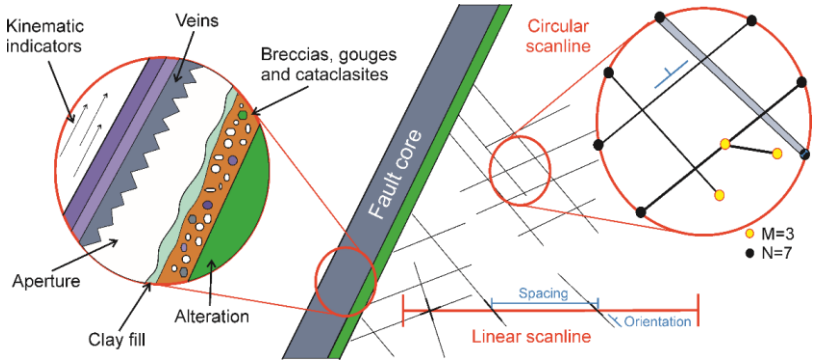


Figure 3: Fault zone schematic with key measurable characteristics and scanline methods. On the circular scanline, fracture terminations (M) and fracture intersections (N) are shown. The plane of scanline surfaces and fractures within scanlines is measured. The characteristics of faults and fractures, shown on the left-hand side, were recorded.

From the linear scanline results, normalized average intensity (P_{10}) was calculated and orientation frequency was plotted, with Terzaghi (1965) corrections applied. From the circular scanline results, size (estimated mean trace length), fracture density (P_{20}) and fracture intensity (P_{21}) estimates were calculated (Rohrbaugh et al., 2002). The accuracy of these estimations is influenced by the number of fracture terminations and intersections (N and M nodes on Figure 3), with 30 recommended for each as a minimum (Rohrbaugh et al., 2002, Watkins et al., 2015). Due to access restrictions, this was impossible for the circular scanlines and therefore the estimations of size, fracture intensity and fracture density are subject to some inaccuracy. For circular scanline PLFZ 3, size could not be calculated as too few nodes were recorded.

3 RESULTS

3.1 Porthgwarra-Land's End Fault Zone

At Pol Ledan, the PLFZ comprises four separate strands over a 100 m wide section, aligning with the estimations of fault zone widths by Yeomans et al. (2023) in the Land's End area of 100–200 m. Fault planes strike WNW–ESE to NW–SE and are all dipping steeply SW (Figure 5). Fault cores are up to 3.1 m wide and comprise several generations of gouge, mechanical breccias, hydrothermal breccias, and quartz–hematite veins (Figure 4). Veins display space-filling epithermal textures (e.g., blocky, elongate blocky, banded microcrystalline; Figure 4d). A fault-parallel tourmaline vein set and a steeply dipping, near-perpendicular NNE–SSW tourmaline vein set are also present. Elongate blocky quartz–hematite veins occasionally preserve apertures up to 2 cm, though most are infilled, while blocky and banded quartz veins lack open space. Hydrothermal breccias are quartz- or hematite-cemented (Figure 4c) and locally exhibit cockade textures. Grain-supported mechanical breccias are cohesive, showing variable cataclasis. Fault gouge with limited cementation occurs in a minor fault core ~100 m from the main fault zone at Porthgwarra (Figure 4b).

Steeply plunging slickenlines are present on the hanging wall fault plane of the northernmost strand (60°/237°) (Figure 4a) and on the footwall fault plane of the southernmost strand (50°/225°). At Porthgwarra, sub-horizontal slickenlines (03°/313°) are visible in the fault gouge on the hanging wall fault plane (Figure 4b).

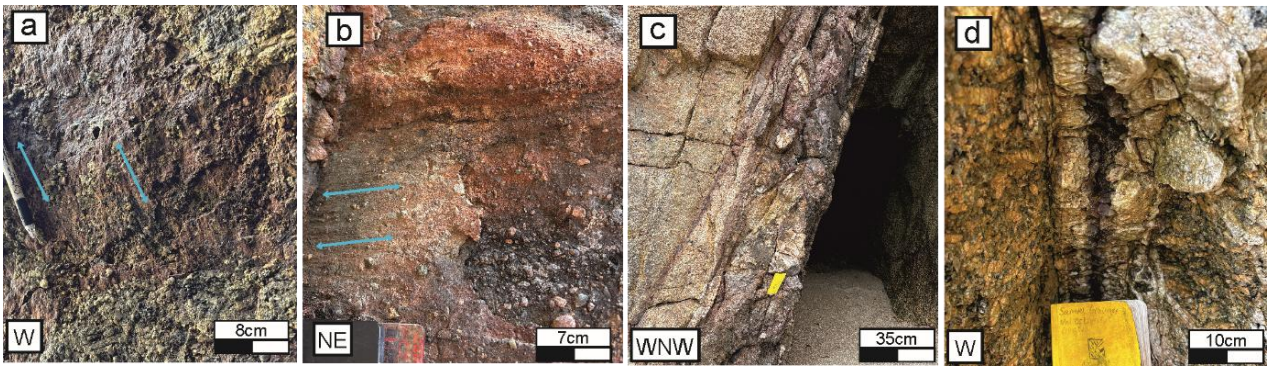


Figure 4: Field photographs, direction of observation given in the bottom left of each figure. a: Steeply inclined slickenlines on the fault surface; b: sub-horizontal slickenlines on a fault gouge slip surface at Porthgwarra; c: Hydrothermal breccia dominated fault core; d: Vein with elongate blocky, syntaxial quartz texture.

3.2 Fractures

Fractures within the fault zone are grouped into four main sets (Figures 5, 7a). The dominant sets strike WNW–ESE and N–S to NNW–SSE and are steeply dipping between 70-90° to the SSW and W, respectively. Both fracture sets are sometimes mineralized. A less common ENE–WSW-striking set dips moderately to steeply to the NW and is rarely mineralized. Finally, gently dipping fractures form a variably oriented set, dominated by N-striking and E-dipping fractures. This set has no occurrences of mineralization. Of the 156 fractures recorded, 20 were mineralized (Figure 5b): one with hematite coating, five with tourmaline, and 14 with quartz ± minor hematite. Tourmaline-filled veins are always crosscut by other fractures and fault planes. Those with quartz mineralization often display similar textures to quartz veins of the fault core. 80.9% of fractures have a width of ≤3 mm, inclusive of mineral fill, 14.6% of fractures have a width ≥10 mm, and 2.5% of fractures have a width ≥100 mm, with the greatest width recorded as 150 mm.

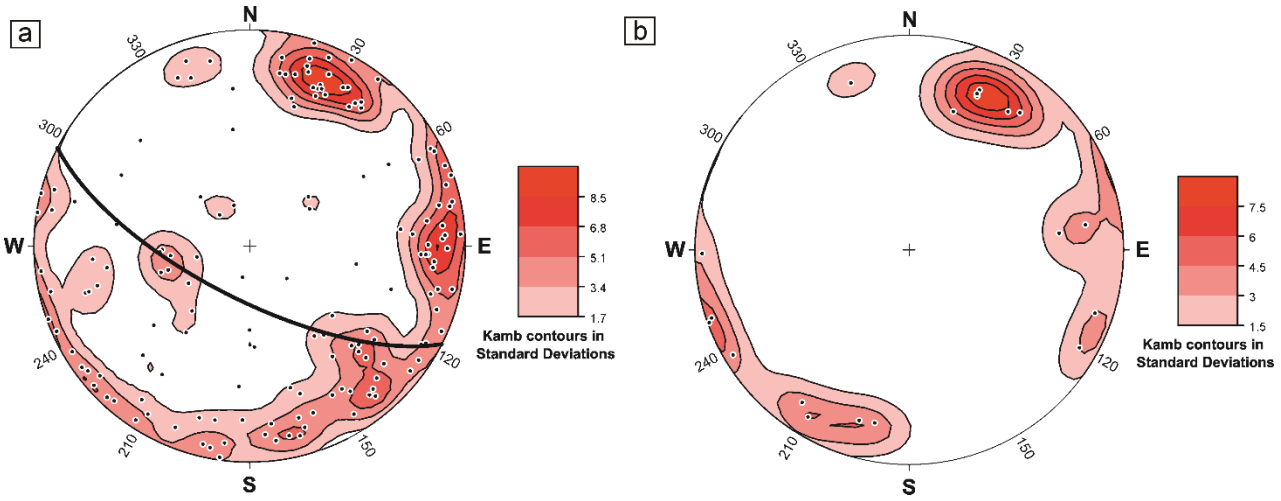


Figure 5: Pi plot of poles to planes of fractures with Kamb contours. a: All fractures. Mean fault orientation represented by the black great circle. b: Mineralized fractures. Plotted using Stereonet 11 (Cardozo and Allmendinger, 2013).

Terzaghi (1965) corrections have been applied to the seven sections of the linear scanline shown in Figure 6. The corrected intensity for the 52.2 m scanline is 3.17 fractures/m. The section with the greatest linear intensity is the immediate hanging wall of the northernmost fault core, which has a linear intensity of 4.91 fractures/m. Using the equations described in Mauldon et al. (2001), fracture intensity, density, and size (mean trace length) were calculated for each circular scanline (Figure 7b).

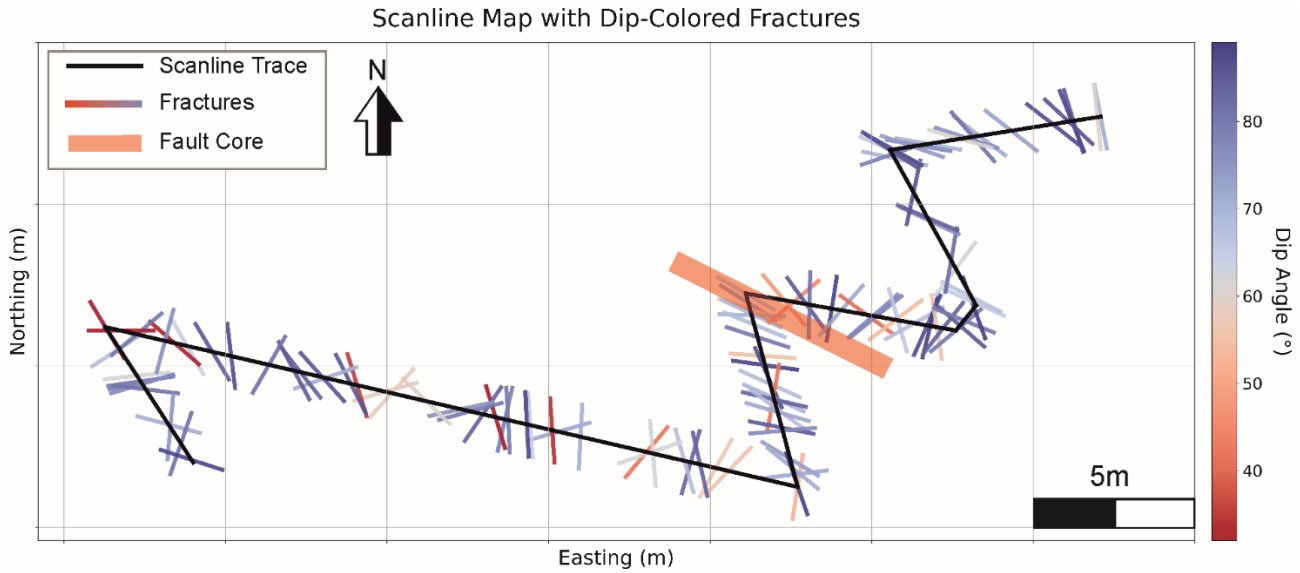


Figure 6: Linear scanline trace with fractures displayed in their true orientation and color coded by dip angle. It is apparent that the exposure traces are mostly fracture controlled, and each section therefore underrepresents fractures of that fracture set.

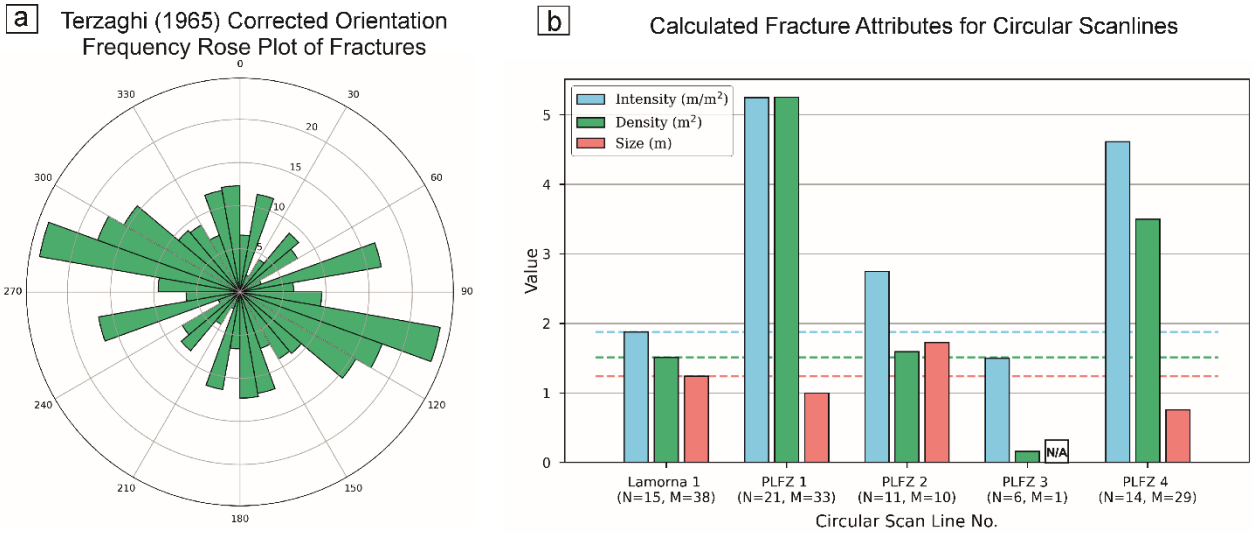


Figure 7: a: Terzaghi corrected strike orientation rose plot for all measured fractures. b: Bar graph showing calculated values of fracture intensity, density, and size from circular scanlines. Lamorna 1 was completed away from any fault zone and represents a 'background' measurement, dashed horizontal lines represent the calculated values from this background dataset. Fracture intersection (N) and fracture termination (M) counts are shown on the X-axis labels.

4 DISCUSSION

4.1 Fault and fracture evolution

The PLFZ displays typical crosscourse fault characteristics as described by other authors (Dominy et al., 1994, Scrivener et al., 1994, Andersen et al., 2016) including epithermal quartz-hematite and breccias. No sulfide or fluorite mineralization was observed in this study. Steeply plunging slickenlines on fault walls indicate oblique-slip kinematics with a dominant extensional component, whilst the Porthgwarra sub-horizontal slickenlines indicate strike-slip kinematics. Multiple generations of vein and breccia textures within fault cores suggest repeated reactivation of the fault strands studied. Fracture intensity and density calculations suggest that faulting has caused increased fracture development in the area forming a damage zone.

Other studies of granites hosting crosscourse faults have identified fault parallel fracture sets (e.g., Reinecker et al., 2021) and background fracturing dominated by subvertical NW–SE-striking and ENE–WSW-striking sets with a less important NE–SW-striking subvertical set and sub-horizontal joints (Pine and Batchelor, 1984). The sub-horizontal fractures identified by other authors are similarly reported as unmineralized (Reinecker et al., 2021, Evans et al., 2025). This fracture set may post-date the flow of mineralizing fluids and may be related to unloading during exhumation or did not support paleo fluid flow.

The fault-parallel WNW–ESE-striking fracture set that dominates the fault damage zone is sometimes mineralized with tourmaline and quartz-hematite whilst the fault cores do not contain tourmaline. Tourmaline mineralization in Southwest England is widely recognized as magmatic, or magmatic-hydrothermal in origin (Jackson et al., 1989, Alderton and Harmon, 1991, LeBoutillier et al., 2002), and associated with Permian emplacement of the Cornubian Batholith (Shail and Simons, 2023). This implies that some WNW–ESE fractures pre-date fault propagation, forming structural weaknesses later exploited in the development of the Porthgwarra-Land's End Fault.

4.2 Fault Permeability

Although the fracture data collected here is subject to some bias, our investigation of the PLFZ permits preliminary interpretations of its permeability characteristics. Significant permeability heterogeneity and anisotropy are inferred within the PLFZ. The presence of thick, mineralized fault cores indicates the fault cores functioned as syn-deformational fluid conduits prior to being sealed, with an initial enhancement of permeability. In the modern system the fault cores are interpreted to serve as barriers to cross-fault fluid flow, as they are bound by impermeable quartz veins. Although usually well cemented, breccias may retain minor permeability (Chester and Logan, 1986, Wibberley et al., 2008) as will the poorly cemented fault gouge. In some cases, fracture propagation and dilation have outpaced fracture healing through precipitation, resulting in aperture preservation along the fault. This aperture may allow the fault core to function as a conduit for along-fault fluid flow. The damage zone, with more intense fracturing that is unmineralized in 87% of occurrences, will

facilitate fluid flow and function as a conduit. In this conceptual model, the fractured damage zone acts as a primary fluid conduit, while the fault core generally inhibits across-fault flow but occasionally permits along-fault flow. Similar permeability architectures have been proposed for many other fault systems (e.g., Caine et al., 1996, Evans et al., 1997, Wibberley et al., 2008, Bense et al., 2013).

The abundant NW–SE-striking, steeply dipping fractures are subject to low normal stresses in the modern stress field and are similarly oriented to the σ_1–σ_2 plane, along which permeability is relatively enhanced (Ferrill et al., 2020). Our results demonstrate that fault architecture exerts a first-order control on permeability anisotropy, with the fault-parallel fractures forming preferential flow pathways under the current NW–SE strike-slip stress regime.

4.3 Implications for geothermal production

The field observations, measurements, and permeability interpretations we have developed as part of this study are of critical importance for commercial reservoir modelling and understanding both geothermal fluids and lithium brine resources. However, to develop them into an effective exploration and project de-risking tool, it is essential they are scrutinized against subsurface observations. For example, whilst target structures at depth likely exhibit similar fracture distributions and fault core characteristics to those mapped here, they may, however, possess a vastly different permeability architecture. This difference is driven by factors such as increased confining pressures (Walsh, 1981) and differing paleo-fluid properties (temperature, composition).

As this project develops, we aim to collaborate with Cornish Lithium to understand these differences. By tying our surface observations to subsurface datasets (e.g., exploration borehole core), we can validate the use of surface fault zones as analogues for deep geothermal systems.

5 CONCLUSIONS AND FUTURE WORK

- The PLFZ provides a well-exposed surface analogue for similar faults targeted at depth for geothermal energy and lithium extraction in Southwest England.
- At Pol Ledan, the fault zone comprises four fault core strands primarily comprising mechanical and hydrothermal breccias, and quartz–hematite veins, while the surrounding damage zone is marked by high fracture intensity and limited mineralization within four dominant fracture sets.
- Structural evidence from fault rocks and slickenlines indicates a multiphase kinematic history with fault displacement in at least two tectonic regimes.
- Permeability across the fault zone is heterogeneous. Fault cores act as barriers to cross-fault flow and potentially permit along-fault fluid flow where aperture is preserved, while the fracture-dense damage zone forms the principal conduit for modern fluid circulation.
- These findings advance understanding of how structural architecture influences fluid flow in geothermal surface analogues, improving predictions of permeability in deeper, fault-controlled geothermal systems.
- Future work will extend this analysis across multiple crosscourse fault zones using outcrop, drone, and drill core datasets to quantify geometric variability and mineralization styles, and to test the validity of surface observations as analogues for the subsurface. The results will be incorporated into Discrete Fracture Network (DFN) models to simulate 3D fracture geometries and assess effective permeability. Complementary microanalytical work will investigate mineral scaling and microstructural evidence for fracture reactivation through time.

Acknowledgments

Work presented here is part of an ongoing PhD study supported by the National Environment Research Council (NERC) TARGET Centre for Doctoral Training (CDT), fully funded by NERC (Grant ref. no. NE/Y005457/1), whose support is gratefully acknowledged. ChatGPT was used to generate Python code for data presentation. I would also like to thank Prof. John Wheeler who has helped supervise this project alongside my co-author supervisors.

6 REFERENCES

ALDERTON, D. & HARMON, R. 1991. Fluid inclusion and stable isotope evidence for the origin of mineralizing fluids in south-west England. *Mineralogical Magazine,* 55**,** 605-611.

ANDERSEN, J. C., STICKLAND, R. J., ROLLINSON, G. K. & SHAIL, R. K. 2016. Indium mineralisation in SW England: host parageneses and mineralogical relations. *Ore Geology Reviews,* 78**,** 213-238.

BAPTIE, B. 2010. Seismogenesis and state of stress in the UK. *Tectonophysics,* 482**,** 150-159.

BARTON, C. A., ZOBACK, M. D. & MOOS, D. 1995. Fluid flow along potentially active faults in crystalline rock. *Geology,* 23**,** 683-686.

BEAMISH, D. & BUSBY, J. 2016. The Cornubian geothermal province: heat production and flow in SW England: estimates from boreholes and airborne gamma-ray measurements. *Geothermal Energy,* 4**,** 4.

BENSE, V. F., GLEESON, T., LOVELESS, S. E., BOUR, O. & SCIBEK, J. 2013. Fault zone hydrogeology. *Earth-Science Reviews,* 127**,** 171-192.

BERTRAND, L., GÉRAUD, Y., LE GARZIC, E., PLACE, J., DIRAISON, M., WALTER, B. & HAFFEN, S. 2015. A multiscale analysis of a fracture pattern in granite: A case study of the Tamariu granite, Catalunya, Spain. *Journal of Structural Geology,* 78**,** 52-66.

CAINE, J. S., EVANS, J. P. & FORSTER, C. B. 1996. Fault zone architecture and permeability structure. *Geology,* 24**,** 1025-1028.

CARDOZO, N. & ALLMENDINGER, R. 2013. Spherical projections with OSXStereonet. *Computers & Geosciences,* 51**,** 193–205.

CHAPMAN, T. 1989. The Permian to Cretaceous structural evolution of the Western Approaches Basin (Melville sub-basin), UK. *Geological Society, London, Special Publications,* 44**,** 177-200.

CHEN, Y., CLARK, A., FARRAR, E., WASTENEYS, H., HODGSON, M. & BROMLEY, A. 1993. Diachronous and independent histories of plutonism and mineralization in the Cornubian Batholith, southwest England. *Journal of the Geological Society,* 150**,** 1183-1191.

CHESTER, F. M. & LOGAN, J. M. 1986. Implications for mechanical properties of brittle faults from observations of the Punchbowl fault zone, California. *pure and applied geophysics,* 124**,** 79-106.

CONNOLLY, J., ANDERSON, M., MOTTRAM, C., PRICE, G. D., PARRISH, R. & SANDERSON, D. 2024. Using U–Pb carbonate dating to constrain the timing of extension and fault reactivation within the Bristol Channel Basin, SW England. *Journal of the Geological Society,* 181**,** jgs2024-021.

DEARMAN, W. 1963. Wrench-faulting in Cornwall and south Devon. *Proceedings of the Geologists' Association,* 74**,** 265-287.

DOMINY, S., SCRIVENER, R., LE BOUTILLIER, N., BUSSELL, M. & HALLS, C. 1994. Crosscourses in South Crofty Mine, Cornwall: further studies of paragenesis and structure. *PROCEEDINGS-USSHER SOCIETY,* 8**,** 237-237.

EVANS, A. J. M., FARRELL, N. J. C., NEAVE, D. A., HARTLEY, M. E., HEALY, D., WATERS, J. P., MCELHINNEY, T. R., SHEA, J. J., BIGARONI, N. & HUNT, S. A. 2025. Fracture analysis of the lithium-bearing Cligga Head granite: Impacts on critical mineral mobilisation and fluid flow. *Journal of Structural Geology***,** 105510.

EVANS, J. P., FORSTER, C. B. & GODDARD, J. V. 1997. Permeability of fault-related rocks, and implications for hydraulic structure of fault zones. *Journal of structural Geology,* 19**,** 1393-1404.

FAULKNER, D., JACKSON, C., LUNN, R., SCHLISCHE, R., SHIPTON, Z., WIBBERLEY, C. & WITHJACK, M. 2010. A review of recent developments concerning the structure, mechanics and fluid flow properties of fault zones. *Journal of Structural Geology,* 32**,** 1557-1575.

FAULKNER, D. R. & ARMITAGE, P. J. 2013. The effect of tectonic environment on permeability development around faults and in the brittle crust. *Earth and planetary science letters,* 375**,** 71-77.

FERRILL, D. A., SMART, K. J. & MORRIS, A. P. 2020. Fault failure modes, deformation mechanisms, dilation tendency, slip tendency, and conduits v. seals. *Geological Society special publication,* 496**,** 75-98.

GLEESON, S., WILKINSON, J., SHAW, H. & HERRINGTON, R. 2000. Post-magmatic hydrothermal circulation and the origin of base metal mineralization, Cornwall, UK. *Journal of the Geological Society,* 157**,** 589-600.

GLEESON, S. A., WILKINSON, J. J., STUART, F. & BANKS, D. 2001. The origin and evolution of base metal mineralising brines and hydrothermal fluids, South Cornwall, UK. *Geochimica et Cosmochimica Acta,* 65**,** 2067-2079.

HOLLOWAY, S. & CHADWICK, R. 1986. The Sticklepath-Lustleigh fault zone: Tertiary sinistral reactivation of a Variscan dextral strike-slip fault. *Journal of the Geological Society,* 143**,** 447-452.

INSKIP, N. F., HARPERS, N., SHAIL, R., CLAES, H., DEN HARTOG, S. & BUSCH, A. 2023. Reservoir properties of fault-related hydrothermally altered granites in Cornwall: Implications for geothermal energy prospectivity. *Authorea Preprints*.

JACKSON, N. J., WILLIS-RICHARDS, J., MANNING, D. A. C. & SAMS, M. S. 1989. Evolution of the Cornubian ore field, Southwest England; Part II, Mineral deposits and ore-forming processes. *Economic Geology,* 84**,** 1101-1133.

KURZ, W., IMBER, J., WIBBERLEY, C. A. J., HOLDSWORTH, R. E. & COLLETTINI, C. 2008. The internal structure of fault zones: fluid flow and mechanical properties. *Geological Society special publication,* 299**,** 1-3.

LEBOUTILLIER, N., CAMM, G., SHAIL, R., BROMLEY, A., JEWSON, C. & HOPPE, N. 2002. Tourmaline-quartz-cassiterite mineralization of the Land's End Granite at Nanjizal, west Cornwall.

LEDINGHAM, P., COTTON, L. & LAW, R. 2019. The united downs deep geothermal power project.

LEVERIDGE, B., HOLDER, M. & GOODE, A. 1990. *Geology of the country around Falmouth*, HM Stationery Office.

LEVERIDGE, B. E. & HARTLEY, A. J. 2006. The Variscan Orogeny: the development and deformation of Devonian/Carboniferous basins in SW England and South Wales.

LIOTTA, D., BROGI, A., RUGGIERI, G. & ZUCCHI, M. 2021. Fossil vs. Active Geothermal Systems: A Field and Laboratory Method to Disclose the Relationships between Geothermal Fluid Flow and Geological Structures at Depth. *Energies,* 14**,** 933.

MAULDON, M., DUNNE, W. & ROHRBAUGH JR, M. 2001. Circular scanlines and circular windows: new tools for characterizing the geometry of fracture traces. *Journal of structural geology,* 23**,** 247-258.

MITCHELL, T. M. & FAULKNER, D. R. 2012. Towards quantifying the matrix permeability of fault damage zones in low porosity rocks. *Earth and Planetary Science Letters,* 339-340**,** 24-31.

NIXON, C. W., SANDERSON, D. J. & BULL, J. M. 2011. Deformation within a strike-slip fault network at Westward Ho!, Devon UK: Domino vs conjugate faulting. *Journal of Structural Geology,* 33**,** 833-843.

OLVER, T. & LAW, R. The United Downs Geothermal Power Plant, Cornwall, UK: combining the generation of geothermal electricity and heat, with the extraction of critical raw materials. Proceedings of the 50th Workshop on Geothermal Reservoir Engineering, Stanford, CA, USA, 2025.

PINE, R. J. & BATCHELOR, A. S. 1984. Downward migration of shearing in jointed rock during hydraulic injections. *International Journal of Rock Mechanics and Mining Sciences & Geomechanics Abstracts,* 21**,** 249-263.

REINECKER, J., GUTMANIS, J., FOXFORD, A., COTTON, L., DALBY, C. & LAW, R. 2021. Geothermal exploration and reservoir modelling of the United Downs deep geothermal project, Cornwall (UK). *Geothermics,* 97**,** 102226.

ROHRBAUGH, JR., DUNNE, W. M. & MAULDON, M. 2002. Estimating fracture trace intensity, density, and mean length using circular scan lines and windows. *AAPG bulletin,* 86**,** 2089-2102.

SANDERSON, D. J. & NIXON, C. W. 2018. Topology, connectivity and percolation in fracture networks. *Journal of Structural Geology,* 115**,** 167-177.

SCRIVENER, R. C., DARBYSHIRE, D. P. F. & SHEPHERD, T. J. 1994. Timing and significance of crosscourse mineralization in SW England. *Journal of the Geological Society,* 151**,** 587-590.

SHAIL, R. & SIMONS, B. 2023. The Cornubian Batholith: Post-Collisional Variscan Granites and Resources. *Metallic Resources 1: Geodynamic Framework and Remarkable Examples in Europe***,** 143-219.

SHAIL, R. K. & ALEXANDER, A. C. 1997. Late Carboniferous to Triassic reactivation of Variscan basement in the western English Channel: evidence from onshore exposures in south Cornwall. *Journal of the Geological Society,* 154**,** 163.

SHAIL, R. K. & LEVERIDGE, B. E. 2009. The Rhenohercynian passive margin of SW England: Development, inversion and extensional reactivation. *Comptes Rendus. Géoscience,* 341**,** 140-155.

SHAW, R. 2022. The potential for lithium in the UK. *In:* LUSTY, P., JOSSO, P. & HILL, A. (eds.).

SIBSON, R. H. 1990. Conditions for fault-valve behaviour. *Deformation Mechanisms, Rheology and Tectonics,* 54**,** 15-28.

SIBSON, R. H. 2000. Fluid involvement in normal faulting. *Journal of geodynamics,* 29**,** 469-499.

SIBSON, R. H. 2001. Seismogenic framework for hydrothermal transport and ore deposition.

TERZAGHI, R. D. 1965. Sources of error in joint surveys. *Geotechnique,* 15**,** 287-304.

TURAN, A., BROWN, C. S., SHAIL, R. & SASS, I. 2024. Probabilistic assessment of deep geothermal resources in the Cornubian Batholith and their development in Cornwall and Devon, United Kingdom. *Geothermics,* 122**,** 103081.

WALSH, J. Effect of pore pressure and confining pressure on fracture permeability. International journal of rock mechanics and mining sciences & geomechanics abstracts, 1981. Elsevier, 429-435.

WATKINS, H., BOND, C. E., HEALY, D. & BUTLER, R. W. 2015. Appraisal of fracture sampling methods and a new workflow to characterise heterogeneous fracture networks at outcrop. *Journal of Structural Geology,* 72**,** 67-82.

WIBBERLEY, C. A. J., YIELDING, G. & TORO, G. D. 2008. Recent advances in the understanding of fault zone internal structure: a review. *Geological Society, London, Special Publications,* 299**,** 5-33.

YEOMANS, C. M., CLARIDGE, H., HUDSON, A. J. L., SHAIL, R. K., WILLEMS, C., EYRE, M. & HARKER, C. 2023. A single multi-scale and multi-sourced semi-automated lineament detection technique for detailed structural mapping with applications to geothermal energy exploration. *Quarterly Journal of Engineering Geology and Hydrogeology,* 56**,** qjegh2022-051.